


Article

# Two-Stage Configuration of User-Side Hybrid Energy Storage Based on Fuzzy Optimization

Yuanxing Xia <sup>1</sup>, Qingshan Xu <sup>1,\*</sup>, Jun Zhao <sup>2</sup> and Chengliang Wang <sup>3</sup><sup>1</sup> School of Electrical Engineering, Southeast University, Nanjing 210096, China; 230198647@seu.edu.cn<sup>2</sup> School of Control Science and Engineering, Dalian University of Technology, Dalian 116024, China; zhaoj@dlut.edu.cn<sup>3</sup> Jiangsu Fangtian Power Technology Co., Ltd., Nanjing 210000, China; cllw@126.com

\* Correspondence: xuqingshan@seu.edu.cn

Received: 24 October 2019; Accepted: 29 November 2019; Published: 5 December 2019



**Abstract:** This paper proposes a new method for configuring hybrid energy storage systems on the user side with a distributed renewable energy power station. To reasonably configure the hybrid energy storage system, this paper divides the whole optimization into two stages from the two dimensions of capacity and power: supercapacitor and battery optimization. To minimize the fluctuation of new energy output when the user's investment is as small as possible, a dual agent fuzzy optimization algorithm is used in the configuration of the supercapacitor. When the battery is configured, the optimization objective is to maximize the user's income and minimize the number of charges and discharges in an optimization cycle. By dividing two objective functions, multi-objective optimization is integrated into single-objective optimization, the battery life is extended, and the total revenue of the user in the whole life cycle is increased.

**Keywords:** hybrid energy storage; user side; fuzzy optimization

## 1. Introduction

Recently, due to the rapid development of the global economy, the power consumption on the user side has increased significantly [1], and the difference between peak and valley loads on the user side is increasing [2,3]. Therefore, with the further expansion of peak-valley difference of users' electricity load, the government has established a two-part tariff system to encourage users to participate actively in load regulation [4]. The electricity charged by the two-part tariff in a charge cycle (CC) is as follows,

$$p = P_{peak} \times a + E \times b \quad (1)$$

where  $P_{peak}$  is the maximum load in the charge cycle,  $a$  is the demand price,  $E$  is the quantity of electricity consumed during the charge cycle, and  $b$  is the energy price.

Due to the increasing depletion of fossil fuels, many high-load industrial users are building photovoltaic power (PV) generation devices on the user side [5,6]. However, PV generation is greatly affected by light intensity and many other environmental factors [7,8], and its output fluctuates obviously. If directly connected to the grid, PV generation will affect the power quality and stability of the grid. Therefore, it is necessary to install energy storage devices (ES) in photovoltaic power generation system to suppress output fluctuations [9].

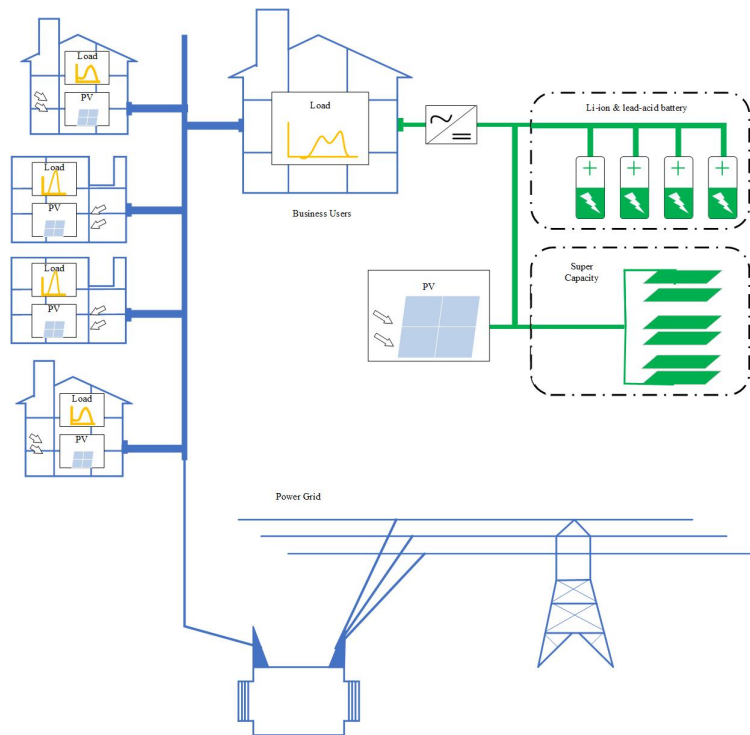


**Figure 1.** Structural chart of user-side photovoltaic hybrid energy storage model.

The power density and energy density when configuring ES on the user side need to be fully considered [10]. This paper establishes a hybrid energy storage model to suppress photovoltaic fluctuations, as shown in Figure 1. The expression of the load after configuration  $P_{loadafter}$  is

$$P_{loadafter} = P_{load} + P_{ES} + P_{PV} \tag{2}$$

where  $P_{load}$  is the original user load,  $P_{ES}$  is the ES output (the discharge is negative, and the charge is positive), and  $P_{PV}$  is the PV output.

In this paper, supercapacitors (SC) are selected as ES with high power density and lithium-ion batteries as ES with high energy density. This form of hybrid energy storage can reduce ES loss [11] and improve the power quality of the grid [12,13]. In [14], ES on the user side were divided into two layers: scheduling and operating. These two layers were optimized separately. R. Xiong et al. [15] proposed three evaluation indicators for the optimal allocation of ES on the user side from an economic point of view. In [16], the probabilistic weighted Markov process was used to predict future loads and determine the charging and discharging strategy based on state trajectory and ES loss. The whole life-cycle cost and benefit of ES were comprehensively considered in [17,18], but the model revenue part was too basic, and peak load reduction was not considered. Hu X. et al. [19] analyzed the pricing strategy under a fixed investment return period on the basis of three different mechanisms, but they did not consider the actual charging and discharging strategy, and the evaluation of the overall value of ES was incomplete.

To summarize, the existing optimal configuration schemes hardly consider prolonging the energy storage life from the point of reducing the number of charging and discharging cycles in each CC. There is seldom reference analyzing the impact of self-built distributed renewable energy generation on user-side ES configurations. Therefore, this paper establishes a two-stage multi-objective optimization model [20]. The optimization objective of the first stage is to suppress the fluctuation of PV output. The optimization objectives of the second stage are increasing the income of users' ES investment and reducing the number of ES actions in each CC. The constraint conditions of this model include the limitation of the number of charging and discharging cycles, the SOC of ES, and the caps on ES investment.

The remainder of this paper is arranged as follows. The SC optimization model (Stage 1) and the large capacity battery optimization model (Stage 2) are introduced in Section 2. A two-stage optimization model based on fuzzy theory is proposed in Section 3. The case analysis is discussed in Section 4. Finally, the conclusion of paper is presented in Section 5.

## 2. Two-Stage Optimization Model of Hybrid Energy Storage on the User-Side

### 2.1. Stage 1: Supercapacitor Configuration

#### 2.1.1. Model of Super Capacitor from the User’s Perspective

Taking the basic reference output as 1000 kW [21], the corresponding curve spectrum is solved by fast Fourier transform. In this paper, three common filtering algorithms are used to filter photovoltaic data: median filter (MF), wavelet transform (WT), and moving average filter (MAF) [22,23]. Because MF is very effective in smoothing impulse noise, it can protect the sharp edge curve of photovoltaic output by selecting the appropriate point to replace the bad point with large fluctuations. [24] MF is selected to process photovoltaic data in this paper. The time and frequency spectra of each waveform are shown in Figure 2. It can be seen from the Figure 2 that among the three filter algorithms, the median filtering output is the smoothest. The proportion of high-frequency components after filtering is shown in Table 1. In this paper, the price of a capacitor per unit capacity is set as  $c_{SC_E}$ , the price of a capacitor per unit power is set as  $c_{SC_P}$ , and then the mathematical model is established from the user’s point of view as follows.

$$Min : C_{invest1} = c_{SC_P} \times P_{SC} + c_{SC_E} \times E_{SC} \tag{3}$$

$$s.t. P_{SC,cha,t} \leq P_{SC} \times B_{SC,cha,t} \tag{4}$$

$$P_{SC,dis,t} \leq P_{SC} \times B_{SC,dis,t} \tag{5}$$

$$B_{SC,dis,t} + B_{SC,cha,t} \leq 1 \tag{6}$$

$$SOC_{SC}(t + 1) = SOC_{SC}(t) - \frac{\eta P_{SC}(t)\Delta t}{E_{SC}} \tag{7}$$

$$SOC_{SCmin} < SOC_{SC} < SOC_{SCmax} \tag{8}$$

$$SOC_{SCinitial} = SOC_{SCfinal} \tag{9}$$

where  $P_{SC}$  is the rated power of SC,  $E_{SC}$  is the rated capacity of SC (discharge is positive, and charge is negative), and  $SOC_{SC}$  is the SOC of SC, which has upper and lower limits of  $SOC_{SCmax}$  and  $SOC_{SCmin}$ , respectively.  $\eta$  is the charge–discharge coefficient,  $\Delta t$  is the time interval.  $B_{SC,cha,t}$  and  $B_{SC,dis,t}$  are boolean variables, representing charge and discharge state constraints,  $B_{SC,dis,t} = 1$  if SC is in the discharge state,  $B_{SC,dis,t} = 0$  if SC is in the charge state, and  $B_{SC,cha,t}$  is the same as  $B_{SC,dis,t}$ . In the optimization model, the objective function indicates that the user wants capacitor investment to be as small as possible, and the constraints indicate that the charging state of the capacitor needs to be kept within the normal range. Capacitor charging and discharging upper limits are determined by the rated power of the capacitor.

Table 1. High-frequency ratio.

Primary Photovoltaic Output	Wavelet Transform	Moving Average Filtering	Median Filtering
0.3981	0.3953	0.3235	0.3197

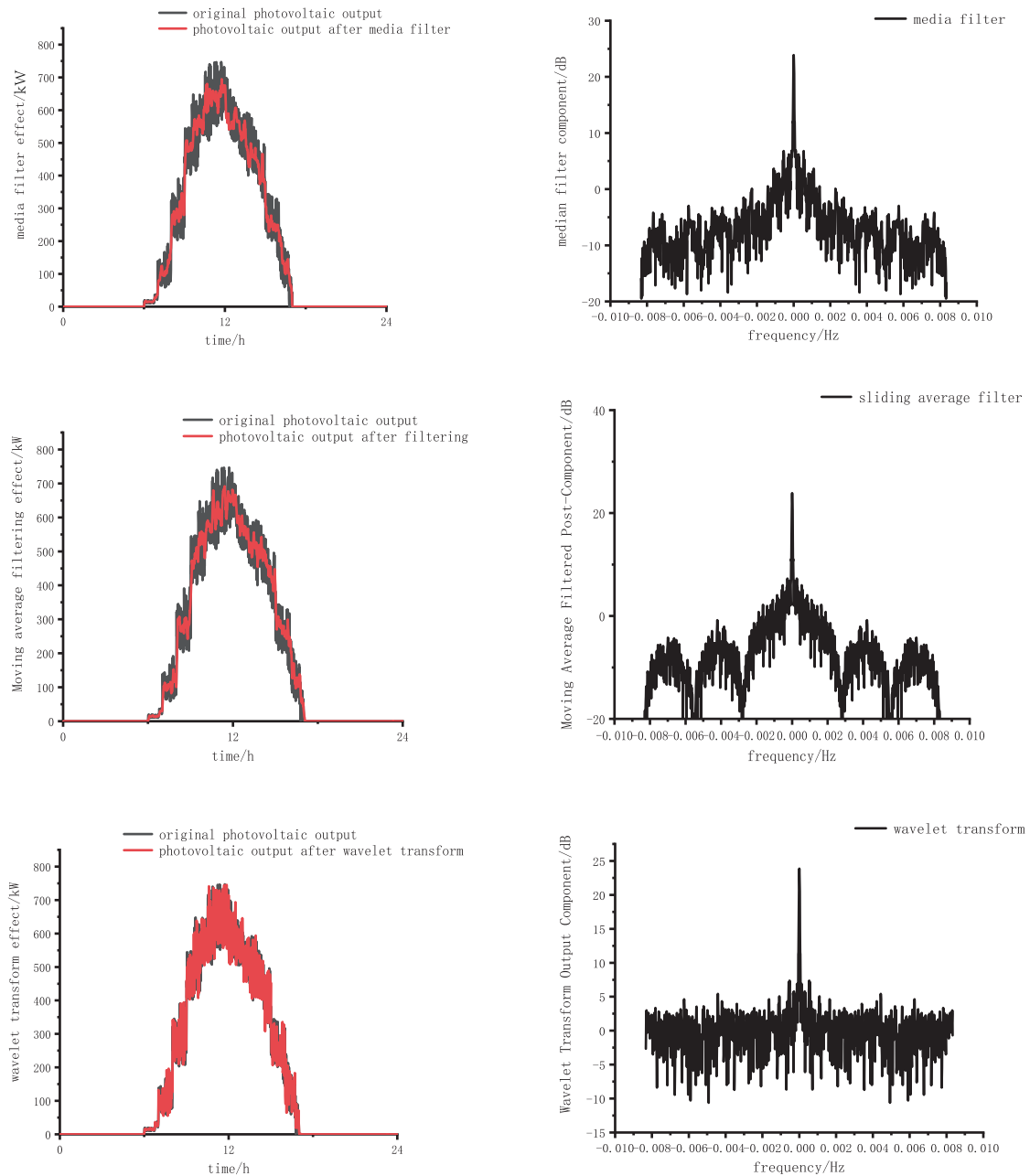


Figure 2. Comparison of three filtering algorithms.

### 2.1.2. Model of Power Quality from Grid’s Perspective

Due to the limitation of investment and operation of SC, it is difficult for SC to achieve the effect of the median filter and ideally suppress the fluctuations in photovoltaic output. Therefore, from the perspective of a power grid, it is necessary to establish a filter index  $R$  to minimize the proportion of high-frequency components in the total output:

$$Min : R = \frac{\sum_{f=f_{smp}, f \neq 0}^{f_{max}} Q_f}{Q_0} \tag{10}$$

where  $Q_f$  is the high-frequency component of filtered output and  $f$  denotes frequency. This index represents the proportion of high-frequency output in the conventional output and minimizes the proportion under the normal operation of capacitors.

### 2.2. Stage 2: Large Capacity Battery Configuration

According to the IEC 600300-3-3 standard [25], under the two-part tariff system, the user's tariff is closely related to the peak load on the grid side during the CC. According formula (2), the grid side load is related to the PV output after stabilization. Therefore, the user's load after PV compensation is used as the underlying optimization parameter to input the battery optimization configuration model for optimization. The optimal allocation model of batteries in the life cycle is as follows.

Maximum total revenue:

$$Max : C_{invest2} = C_{inc} + C_{rec} - C_{invest} - C_{maintain} \tag{11}$$

Minimum number of charging and discharging cycles:

$$Min : N = \sum_{t=1}^T B_{cha}(t) + \sum_{t=1}^T B_{dis}(t) \tag{12}$$

Energy storage scheduling revenue can be divided into demand and cost savings:

$$C_{inc} = C_{need} + C_{strategy} \tag{13}$$

$$C_{strategy} = \sum_{y=1}^Y \sum_{day=1}^{DAY} \left( \sum_{t=1}^T d(t) (P_{dis,day,y}(t) - P_{cha,day,y}(t)) \Delta t \right) \left( \frac{1+i}{1+d} \right)^y \tag{14}$$

$$C_{need} = \sum_{y=1}^Y \left( \sum_{m=1}^M (\alpha * \delta P_{peak,m,y}) \right) \left( \frac{1+i}{1+d} \right)^y \tag{15}$$

Energy storage recovery income:

$$C_{rec} = \beta C_{invest} \tag{16}$$

Investment cost of energy storage:

$$C_{invest} = c_P P_{max} + c_E E_{max} \tag{17}$$

Energy storage operation and maintenance cost:

$$C_{maintain} = \sum_{y=1}^Y (C_m P_{max}) \left( \frac{1+i}{1+d} \right)^y \tag{18}$$

Constraint condition:

$$s.t. \quad C_{invest} \leq C_{investmax} \tag{19}$$

$$load_{after} = load - output_{pv} \tag{20}$$

$$load_{after} - P_{dis} + P_{cha} \leq (1 - \delta) P_{peak,m,y} \tag{21}$$

$$0 \leq P_{dis}(t) \leq P_{max} B_{dis}(t) \tag{22}$$

$$0 \leq P_{cha}(t) \leq P_{max} B_{cha}(t) \tag{23}$$

$$B_{dis}(t) + B_{cha}(t) \leq 1 \tag{24}$$

$B$  denotes the state of charge and discharge.  $B_{dis} = 1$  if energy storage is in the discharge state,  $B_{dis} = 0$  if energy storage is in the charge state, and  $B_{cha}$  is the same as  $B_{dis}$ . Therefore, the sum of these two boolean variables can be used to calculate the total number of charging and discharging cycles.

$$SOC_{min} < SOC_{battery} < SOC_{max} \tag{25}$$

$$SOC_{battery,initial,m} = SOC_{battery,final,m} \tag{26}$$

$$SOC_{battery}(t) = SOC_{battery}(t - 1) + \frac{[\eta^{cha} P_{cha}(t) - P_{dis}(t) / \eta^{dis}] \Delta t}{E_{max}} \tag{27}$$

where  $C_{inc}$  represents the benefit of peak-valley arbitrage,  $C_{strategy}$ , and demand savings  $C_{need}$ ,  $C_{rec}$  is the revenue of recycling energy storage;  $C_{invest}$  represents the energy storage investment;  $C_{maintain}$  represents the cost of energy storage operation and maintenance;  $P_{dis,day,y}$  denotes the discharge power of energy storage on the day-th day of the y-th year; and  $P_{cha,day,y}$  denotes energy storage charging power.  $\alpha$  represents electricity demand price,  $\delta$  denotes peak shaving rate,  $P_{peak,m,y}$  represents the peak value of the original load in the m-th month of the y-th year.  $i$  denotes inflation rate, and  $d$  denotes the discount rate.  $P_{max}$  denotes the rated battery power, and  $E_{max}$  represents the rated capacity of the battery.  $d(t)$  denotes the peak-valley time-of-use tariff at t-time.  $\eta$  denotes the charge–discharge coefficient. The SOC constraints of the batteries are consistent with the SOC constraints of the supercapacitors.

### 3. Two-Stage Optimization Algorithm Based on Fuzzy Optimization

#### 3.1. Multi-Objective Fuzzy Optimization

In the above model, there are two competing objective functions, and it is impossible for both of them to achieve the optimum at the same time. For the multi-objective programming problem, it is advisable to use the theory of fuzzy sets to transform the problem into a single-objective problem. On the premise of satisfying all constraints, considering user investment and smoothing photovoltaic output, the total cost of investing in supercapacitors and the total proportion of high-frequency components in the output need to be as small as possible. There is an upper limit and no lower limit in these two objectives. Therefore, the reduced half-line is chosen as their membership function, as shown in Figure 3. In the membership function, the ordinate represents the satisfaction of each subject (i.e., grid and user) and the abscissa represents the index of each subject. It can be seen from Figure 3 that the main body will eventually reach the most satisfactory level.

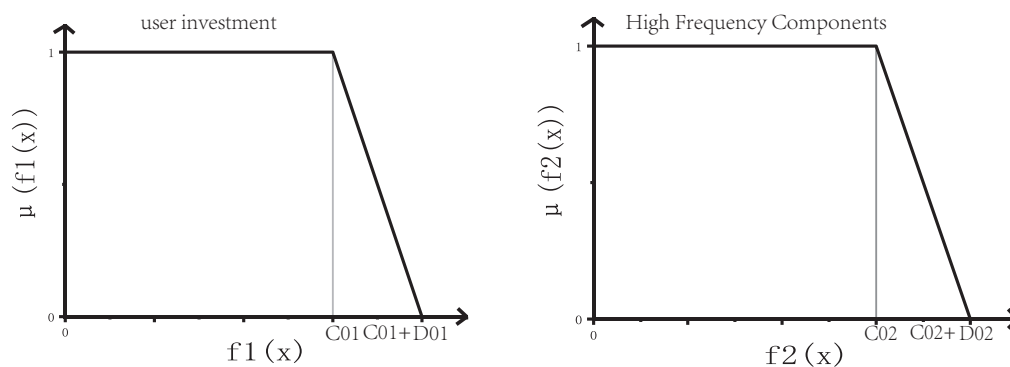


Figure 3. Membership function of two optimization objectives.

Two membership functions can be expressed as

$$\mu(f_1(x)) = \begin{cases} 1, & \text{if } f_1(x) < C01; \\ \frac{C01+D01-f_1(x)}{D01}, & \text{if } C01 \leq f_1(x) \leq C01 + D01; \\ 0, & \text{if } f_1(x) > C01 + D01. \end{cases} \quad (28)$$

$$\mu(f_2(x)) = \begin{cases} 1, & \text{if } f_2(x) < C02; \\ \frac{C02+D02-f_2(x)}{D02}, & \text{if } C02 \leq f_2(x) \leq C02 + D02; \\ 0, & \text{if } f_2(x) > C02 + D02. \end{cases} \quad (29)$$

where C01 is the result when the minimum investment of users is taken as the optimization objective, C02 is the result when the smoothest photovoltaic output is considered separately, C01 + D01 is the maximum acceptable value for user investment, and C02 + D02 is the maximum allowable value for the proportion of high-frequency components in the PV output. Taking  $\lambda$  as the smallest subordinate variable in all subordinate functions, satisfaction can be expressed as

$$\lambda = \text{Min} : \{\mu(f_1(x)), \mu(f_2(x))\} \quad (30)$$

According to the principle of maximum membership degree, the original multi-objective optimal allocation problem can be transformed into a membership degree that satisfies all constraints, i.e., satisfaction maximum. At this time, the optimization results will comprehensively satisfy of both users and grids and can be simply represented by the following models.

$$\text{Min} : -\lambda \quad (31)$$

$$\text{s.t. } C01 \leq f_1(x) + D01 * \lambda \leq C01 + D01 \quad (32)$$

$$C02 \leq f_2(x) + D02 * \lambda \leq C02 + D02 \quad (33)$$

$$0 \leq \lambda \leq 1 \quad (34)$$

Supercapacitor Operation Constraints: (4)–(9).

### 3.2. Two-Stage Optimization Algorithm Based on GUROBI

In summary, the specific steps of the two-stage algorithm for optimizing the configuration in this paper are as follows.

- Step 1: Input photovoltaic output data and load data
- Step 3: Determine whether the fluctuation of output data meets the grid-connected requirements, and if it meets the requirements, move to step 5. If not, adjust the fuzzy parameters, increase the investment of the supercapacitor, and return to step 2 to recalculate the filtering effect.
- Step 3: If the requirement is not met, calculate the fuzzy parameters from the viewpoint of users and power grid.
- Step 4: Establish a fuzzy optimization model to optimize the configuration of supercapacitors, verify whether the photovoltaic output after capacitance configuration meets the requirements, and return to step 2 if it does not meet the requirements.
- Step 5: Calculate user loads with the superimposed photovoltaic output if the requirements are met.
- Step 6: According to the overlapped load, establish the optimal battery allocation model under a two-part tariff.
- Step 7: Use *GUROBI* to solve the model and obtain the optimal configuration scheme of hybrid energy storage in the photovoltaic scenario.

**Remark 1.** To achieve the two goals of reducing charging and discharging cycles and improving the user’s income, rewrite the battery optimization target as follows.

$$Max : \frac{C_{invest2}}{N} \tag{35}$$

**Remark 2.** To successfully solve the problem with GUROBI, as many nonlinear terms in the objective function need to be removed as possible. Therefore, the inflation term in objective functions (14), (15), and (18) is removed to simplify the optimization process. After the optimization, the results are added for analysis.

#### 4. Case Study

The year-round load data of heavy-duty industrial users in Jiangsu Province China are chosen as an example in this paper. The specifications of batteries and supercapacitors are shown in Table 2. To simplify the model, it is assumed that the batteries are continuously optimized and that the supercapacitors are discretely optimized. The parameters of a supercapacitor are selected as Table 3, and the price of SC is CNY1218. The charge of unit electricity of demand is 40 CNY/(kW · month). The time-of-use tariff is consistent with the current system in Jiangsu.

**Table 2.** Relative parameters of the energy storage system.

Performance Index	Battery	Super Capacity
Power Cost Coefficient (CNY/kW)	1500	1500
Capacity Cost Coefficient (CNY/kWh)	1000	27000
Operation Cost Coefficient (CNY/kW)	0.05	0.05
Charging and discharging efficiency	0.85	0.95
Range of SOC	(0.2, 0.8)	(0.1, 0.9)

**Table 3.** Selected supercapacitor parameters.

Specification Parameter	Numerical Value
Capacity (F)	10
Rated voltage (V)	5
Rated current (A)	40
Rated power (kW)	0.2
Rated capacity (kWh)	0.034

##### 4.1. Optimal Allocation of SC

- (1) Input the PV output data, load data, and SC price data, calculate the proportion of PV output in the total load output and SC charging and discharging behavior after MF, and obtain the minimum investment cost C01 of SC, the maximum investment cost  $f1max$  of SC, and the high-frequency component strength after filtering.
- (2) Input the PV output data, load data and SC price data; calculate the PV output spectrum after MF and the original spectrum of PV output; and obtain the minimum allowable high-frequency ratio C02 of PV output, the maximum high-frequency ratio  $f2max$  of PV output, and the corresponding SC investment.
- (3) According to  $D01 = f1max - C01$  and  $D02 = f2max - C02$ , substitute D01 and D02 into formulas (25) and (26) to obtain the membership functions, and the multi-objective optimization problems of users and power grids can be transformed into single-objective optimization. Satisfaction can be obtained using GUROBI as Table 4.



**Table 4.** Maximum satisfaction index and optimized results.

$\lambda$	$\lambda(f1)$	$\lambda(f2)$	$f1(CNY \times 10^4)$	$f2$
0.39	0.96	0.39	28.796	0.39
0.73	0.73	0.96	41.412	0.33
0.52	0.94	0.52	30.45	0.37
0.82	0.82	0.86	36.54	0.34

#### 4.2. Optimal Allocation of Batteries

The battery configuration corresponding to the maximum load is chosen to optimize the user’s load for the whole year of 2017. The upper limit of the number of battery charging and discharging cycles is set to 4000. The results of the investments and returns of users in the life cycle are shown in Table 5.

**Table 5.** Total investment results.

Project	Economic Performance
Total Investment (CNY $\times 10^4$ )	396.54
Super Capacitor Investment (CNY $\times 10^4$ )	36.5
Battery Investment (CNY $\times 10^4$ )	360.04
Operation and Maintenance Investment (CNY $\times 10^4$ )	0.504
Total revenue (CNY $\times 10^4$ )	746.05
Income share of demand savings	34.63 %
Years of Return on Investment (year)	7.49
Annual return on investment	12.5 %
Annual average cycle times of charge and discharge	377

#### 4.3. Discussion

According to the results of fuzzy optimization, the optimum degree of satisfaction is 0.82, and 296 supercapacitors need to be configured at this time. The corresponding output curve is shown in Figure 4. The curve of satisfaction of the two objectives with capacitance investment is shown in Figure 4. Figure 5 shows that due to the investment limitation of SC, there are upper and lower limits of SC output, which cannot fully achieve the effect of MF. The intersection of Figure 5 is the optimal configuration point that satisfies the grid and users.

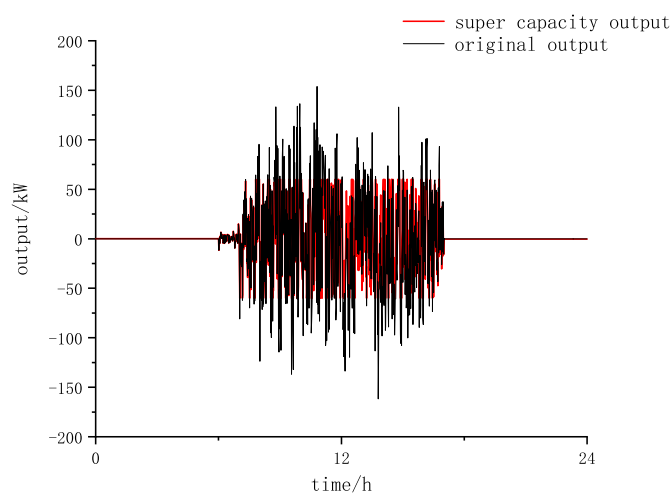


**Figure 4.** SC output.

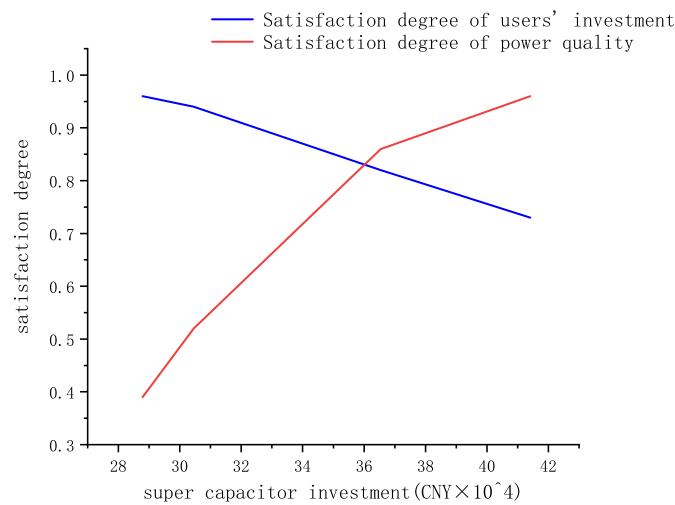


Figure 5. Satisfaction degree.

In this paper, the typical daily load of the industrial user for 12 months is selected by a clustering algorithm.

The large daily load, medium daily load and small daily load of these 12 typical daily loads are selected and optimized, respectively. The output curves of the three kinds of loads are shown in Figures 6–8. It can be seen from the figure that the peak load after energy storage adjustment was successfully reduced by 10–20%, and the energy storage was charged to reduce the overall electricity price in the late night and other low price periods.

According to the configuration results, the larger the load level is, the larger the energy storage specifications that need to be configured. Therefore, the battery configuration corresponding to the maximum load was chosen to optimize the user’s load for the whole year of 2017.

The industrial user selected in this paper shows obvious characteristics of working and non-working days. By reducing the maximum load requirement of each month, this model reduces the monthly electricity demand and improves the user’s income. Under the current hourly tariff background, the cost can be recovered after installing hybrid energy storage for 7.5 years, which shows that the model has application value and popularization significance.

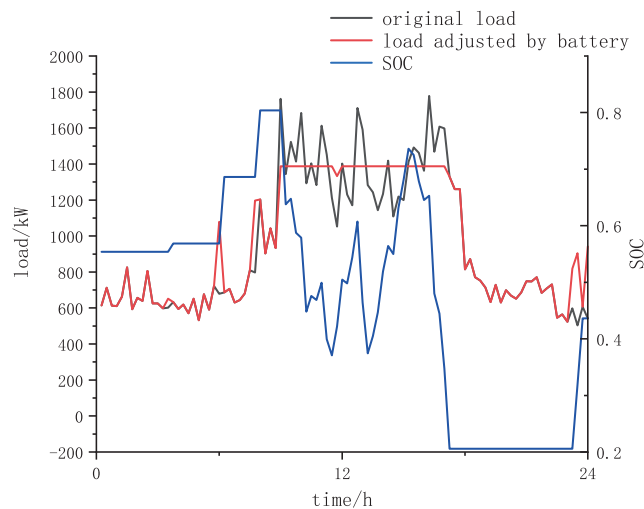
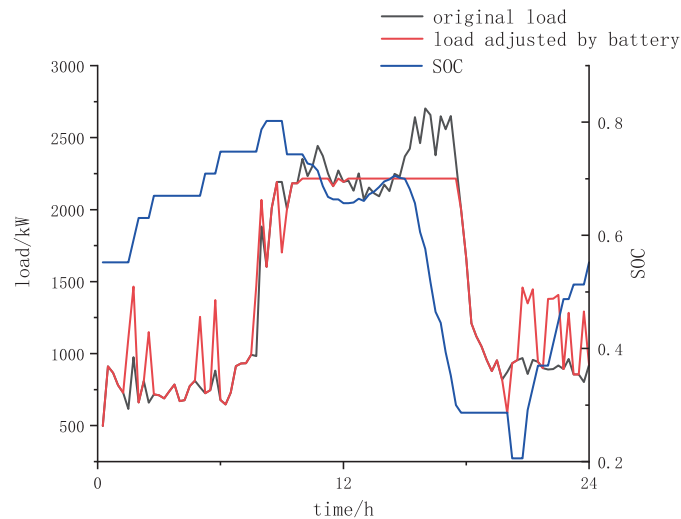
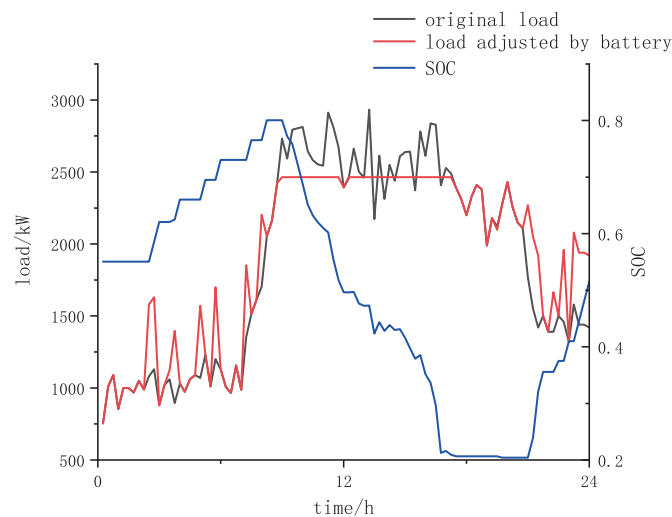


Figure 6. Energy storage configuration for minimum load.



**Figure 7.** Energy storage configuration for medium load.



**Figure 8.** Energy storage configuration for maximum load.

Because the non-working day load has no peak and does not require energy storage regulation, the number of energy storage charging and discharging cycles throughout the year is greatly reduced. With that load characteristic, the average energy storage only needs 377 cycles in 2017, which achieves the target of minimizing the number of charge and discharge cycles so that the energy storage can be used for 10.61 years in total.

## 5. Conclusions

In this application scenario, supercapacitors are used to suppress the fluctuation of photovoltaic output, and batteries are used to reduce the user's maximum load demand. The characteristics of this model are as follows.

- (1) This paper uses fuzzy optimization theory to optimize capacitor configuration from two aspects of power grid and users. Considering the benefits of users and the stability of the power grid, it can be seen from the calculation examples that both sides reach a more satisfactory state.
- (2) The whole multi-objective optimization process is divided into two stages to make the optimization process clear. In the second stage, the multi-objective optimization uses the method of dividing objective functions to ensure the user's benefit and reduce the number of charging and discharging cycles in each CC, to improve the service life of energy storage. It can be seen from the calculation results that ES life is extended to 10.61 years after the number of CCs is

determined, which successfully compensates for the investment and operation cost of ES systems and enables users to make profits.

**Author Contributions:** Conceptualization, Y.X.; methodology, Y.X. and Q.X.; software, Y.X.; validation, Y.X.; formal analysis, J.Z. and C.W.; writing—original draft preparation, Y.X.; writing—review and editing; supervision, Q.X.; project administration, Q.X.; funding acquisition, Q.X.

**Funding:** This research was funded by Chinese National Natural Science Foundation, grant number 51936003 and Chinese National Natural Science Foundation, grant number 51877044.

**Conflicts of Interest:** The authors declare no conflicts of interest.

## Abbreviations

The following abbreviations are used in this manuscript.

SC	supercapacitor
cha	charge
dis	discharge
CNY	Chinese Yuan
CC	Charge Cycle
PV	Photovoltaic
ES	Energy Storage
MF	Median Filter
WT	Wavelet Transform
MAF	Moving Average Filter
SOC	State of Charge

## References

- Jiang, W.; Zhang, L.; Zhao, H.; Hu, R.; Huang, H. Research on power sharing strategy of hybrid energy storage system in photovoltaic power station based on multi-objective optimization. *IET Renew. Power Gener.* **2016**, *10*, 575–583. [[CrossRef](#)]
- Jayasekara, N.; Masoum, M.A.S.; Wolfs, P.J. Optimal operation of distributed energy storage systems to improve distribution network load and generation hosting capability. *IEEE Trans. Sustain. Energy* **2016**, *7*, 250–261. [[CrossRef](#)]
- Zhang, X.; Yuan, Y.; Hua, L.; Cao, Y.; Qian, K. On generation schedule tracking of wind farms with battery energy storage systems. *IEEE Trans. Sustain. Energy* **2017**, *8*, 341–353. [[CrossRef](#)]
- Yan, W.; Sheng, L.; Xu, D.; Yang, W.; Liu, Q. H $\infty$  robust load frequency control for multi-area interconnected power system with hybrid energy storage system. *Appl. Sci.* **2018**, *8*, 1748. [[CrossRef](#)]
- Yan, N.; Zhang, B.; Li, W.; Ma, S. Hybrid energy storage capacity allocation method for active distribution network considering demand side response. *IEEE Trans. Appl. Superconduct.* **2018**, *29*, 1–4. [[CrossRef](#)]
- Kazemi, M.; Zareipour, H. Long-term scheduling of battery storage systems in energy and regulation markets considering battery's lifespan. *IEEE Trans. Smart Grid* **2018**, *9*, 6840–6849. [[CrossRef](#)]
- Pantic, L.S.; Pavlović, T.M.; Milosavljević, D.D.; Radonjic, I.S.; Radovic, M.K.; Sazhko, G. The assessment of different models to predict solar module temperature, output power and efficiency for nis, serbia. *Energy* **2016**, *109*, 38–48. [[CrossRef](#)]
- Zhang, R.; Mirzaei, P.A.; Carmeliet, J. Prediction of the surface temperature of building-integrated photovoltaics: Development of a high accuracy correlation using computational fluid dynamics. *Sol. Energy* **2017**, *147*, 151–163. [[CrossRef](#)]
- Zidar, M.; Georgilakis, P.S.; Hatziaergyriou, N.D.; Capuder, T.; Škrlec, A. Review of energy storage allocation in power distribution networks: Applications, methods and future research. *IET Gener. Transm. Distrib.* **2016**, *10*, 645–652. [[CrossRef](#)]
- del Granado, P.C.; Pang, Z.; Wallace, S.W. Synergy of smart grids and hybrid distributed generation on the value of energy storage. *Appl. Energy* **2016**, *170*, 476–488. [[CrossRef](#)]
- Kim, W.-W.; Shin, J.-S.; Kim, J.-O. Operation strategy of multi-energy storage system for ancillary services. *IEEE Trans. Power Syst.* **2017**, *32*, 4409–4417. [[CrossRef](#)]

12. Mohammadi, S.; Mohammadi, A. Stochastic scenario-based model and investigating size of battery energy storage and thermal energy storage for micro-grid. *Int. J. Electr. Power Energy Syst.* **2014**, *61*, 531–546. [[CrossRef](#)]
13. Shang, C.; Srinivasan, D.; Reindl, T. An improved particle swarm optimisation algorithm applied to battery sizing for stand-alone hybrid power systems. *Int. J. Electr. Power Energy Syst.* **2016**, *74*, 104–117. [[CrossRef](#)]
14. Song, Z.; Zhang, X.; Li, J.; Hofmann, H.; Ouyang, M.; Du, J. Component sizing optimization of plug-in hybrid electric vehicles with the hybrid energy storage system. *Energy* **2018**, *144*, 393–403. [[CrossRef](#)]
15. Xiong, R.; Cao, J.; Yu, Q. Reinforcement learning-based real-time power management for hybrid energy storage system in the plug-in hybrid electric vehicle. *Appl. Energy* **2018**, *211*, 538–548. [[CrossRef](#)]
16. Yorino, N.; Abdillahi, M.; Sasaki, Y.; Zoka, Y. Robust power system security assessment under uncertainties using bi-level optimization. *IEEE Trans. Power Syst.* **2018**, *33*, 352–362. [[CrossRef](#)]
17. Hesse, H.; Martins, R.; Musilek, P.; Naumann, M.; Truong, C.; Jossen, A. Economic optimization of component sizing for residential battery storage Systems. *Energies* **2017**, *10*, 835. [[CrossRef](#)]
18. Merei, G.; Moshövel, J.; Magnor, D.; Sauer, D.U. Optimization of self-consumption and techno-economic analysis of pv-battery systems in commercial applications. *Appl. Energy* **2016**, *168*, 171–178. [[CrossRef](#)]
19. Hu, X.; Moura, S.J.; Murgovski, N.; Egardt, B.; Cao, D. Integrated ptimization of battery sizing, charging, and power management in plug-in hybrid electric vehicles. *IEEE Trans. Control Syst. Technol.* **2015**, *24*, 1036–1043. [[CrossRef](#)]
20. Sinha, A.; Malo, P.; Deb, K. A review on bilevel optimization: From classical to evolutionary approaches and applications. *IEEE Trans. Evol. Comput.* **2018**, *22*, 276–295. [[CrossRef](#)]
21. Erdinc, O.; Paterakis, N.G.; Pappi, I.N.; Bakirtzis, A.G.; Catalão, J.P.S. A new perspective for sizing of distributed generation and energy storage for smart households under demand response. *Appl. Energy* **2015**, *143*, 26–37. [[CrossRef](#)]
22. Leitermann, O.; Kirtley, J.L. Energy storage for use in load frequency control. In Proceedings of the 2010 IEEE Conference on Innovative Technologies for an Efficient and Reliable Electricity Supply, Waltham, MA, USA, 27–29 September 2010; pp. 292–296.
23. Lv, P.; Liu, C.; Rao, Z. Experiment study on the thermal properties of paraffin/kaolin thermal energy storage form-stable phase change materials. *Appl. Energy* **2016**, *182*, 475–487. [[CrossRef](#)]
24. Sanny, A.; Prasanna, V.K. Energy-efficient median filter on fpga. In Proceedings of the 2013 International Conference on Reconfigurable Computing and FPGAs (ReConFig), Waltham, MA, USA, 27–29 September 2013; pp. 1–8.
25. Linssen, J.; Stenzel, P.; Fleer, J. Techno-economic analysis of photovoltaic battery systems and the influence of different consumer load profiles. *Appl. Energy* **2017**, *185*, 2019–2025. [[CrossRef](#)]



© 2019 by the authors. Licensee MDPI, Basel, Switzerland. This article is an open access article distributed under the terms and conditions of the Creative Commons Attribution (CC BY) license (<http://creativecommons.org/licenses/by/4.0/>).